



# The fate of NO<sub>x</sub> emissions due to nocturnal oxidation at high latitudes: 1-D simulations and sensitivity experiments

P. L. Joyce<sup>1,2</sup>, R. von Glasow<sup>3</sup>, and W. R. Simpson<sup>1,2</sup>

<sup>1</sup>Department of Chemistry and Biochemistry, University of Alaska, Fairbanks, AK, USA

<sup>2</sup>Geophysical Institute, University of Alaska, Fairbanks, AK, USA

<sup>3</sup>Centre for Ocean and Atmospheric Sciences, School of Environmental Sciences, University of East Anglia, Norwich, UK

Correspondence to: W. R. Simpson (wrsimpson@alaska.edu) and R. von Glasow (r.von-glasow@uea.ac.uk)

Received: 29 January 2014 – Published in Atmos. Chem. Phys. Discuss.: 18 March 2014

Revised: 6 June 2014 – Accepted: 13 June 2014 – Published: 29 July 2014

## Abstract.

The fate of nitrogen oxide pollution during high-latitude winter is controlled by reactions of dinitrogen pentoxide (N<sub>2</sub>O<sub>5</sub>) and is highly affected by the competition between heterogeneous atmospheric reactions and deposition to the snowpack. MISTRA (MIcrophysical STRAtus), a 1-D photochemical model, simulated an urban pollution plume from Fairbanks, Alaska to investigate this competition of N<sub>2</sub>O<sub>5</sub> reactions and explore sensitivity to model parameters. It was found that dry deposition of N<sub>2</sub>O<sub>5</sub> made up a significant fraction of N<sub>2</sub>O<sub>5</sub> loss near the snowpack, but reactions on aerosol particles dominated loss of N<sub>2</sub>O<sub>5</sub> over the integrated atmospheric column. Sensitivity experiments found the fate of NO<sub>x</sub> emissions were most sensitive to NO emission flux, photolysis rates, and ambient temperature. The results indicate a strong sensitivity to urban area density, season and clouds, and temperature, implying a strong sensitivity of the results to urban planning and climate change. Results suggest that secondary formation of particulate (PM<sub>2.5</sub>) nitrate in the Fairbanks downtown area does not contribute significant mass to the total PM<sub>2.5</sub> concentration, but appreciable amounts are formed downwind of downtown due to nocturnal NO<sub>x</sub> oxidation and subsequent reaction with ammonia on aerosol particles.

## 1 Introduction

The high-latitude winter is a unique chemical environment characterized by extreme cold, extended periods of darkness, and constant snow cover. As the world's population in-

creases, high latitudes are likely to see increased population, enhanced urbanization, and increased resource extraction, all leading to increased pollution emissions including nitrogen-containing species. Anthropogenic nitric oxide (NO) emissions react to form nitrogen dioxide (NO<sub>2</sub>), and together they form the chemical family of NO<sub>x</sub>, which is ultimately removed through further oxidation to form nitric acid (HNO<sub>3</sub>). Nitric acid can acidify aerosol particles in the atmosphere or deposit to the ground where it has been found to affect ecosystems adversely (Fenn et al., 2003). In sunlit conditions, the principal removal pathway of NO<sub>2</sub> is reaction with OH (Seinfeld and Pandis, 2006) which can form significant amounts of HNO<sub>3</sub> during the day, particularly in polluted regions (Finlayson-Pitts and Pitts, 2000). In the absence of photolysis, the “dark” reaction pathway forms the intermediate species nitrate radical (NO<sub>3</sub>) and dinitrogen pentoxide (N<sub>2</sub>O<sub>5</sub>), which have both been measured in the nocturnal boundary layer (e.g., Brown et al., 2003; Wood et al., 2005; Ayers and Simpson, 2006; Osthoff et al., 2008; Chang et al., 2011; Riedel et al., 2012; Wagner et al., 2013). The dark reaction pathway includes Reactions (R1) to (R3), followed by either Reaction (R4a) or (R4b):



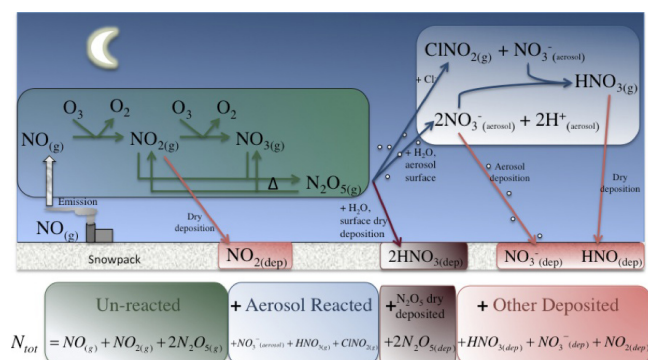


**Figure 1.** A nocturnal nitrogen schematic with emphasis on N<sub>2</sub>O<sub>5</sub> reactivity. The total nitrogen equation (N<sub>tot</sub>) is a sum of the total column-integrated nitrogen from emitted NO<sub>x</sub>, divided into speciation fractions.

The absence of photolysis allows NO<sub>3</sub> to exist in sufficient concentration for Reaction (R3) to occur, and cold temperatures hinder the dissociation of N<sub>2</sub>O<sub>5</sub>, making the cold and dark conditions of high-latitude winter ideal for N<sub>2</sub>O<sub>5</sub> formation. Upon formation, N<sub>2</sub>O<sub>5</sub> can undergo heterogeneous hydrolysis through Reaction (R4a) on the surface of an aerosol particle in the atmosphere or the snowpack surface on the ground to form HNO<sub>3</sub>. Alternatively, N<sub>2</sub>O<sub>5</sub> can react with Cl<sup>-</sup> (Reaction R4b) after uptake in an aerosol particle to form nitryl chloride (ClNO<sub>2</sub>), which is volatile and quickly enters the gas phase. Figure 1 outlines the dark oxidation pathway reaction sequence and the competing removal of N<sub>2</sub>O<sub>5</sub> by reactions on aerosol particles and the snowpack. Cold and dark conditions of high-latitude winter encourage loss of NO<sub>x</sub> via the dark oxidation pathway. In a modeling study, Dentener and Crutzen (1993) found that 80 % of high latitude NO<sub>x</sub> is lost through the dark oxidation pathway in winter. Measurements by Wood et al. (2005) at midlatitudes found that total HNO<sub>3</sub> produced by N<sub>2</sub>O<sub>5</sub> hydrolysis during the night can be comparable to ambient NO<sub>2</sub> concentrations, suggesting total HNO<sub>3</sub> produced by heterogeneous hydrolysis may be greater at high latitudes during winter.

The probability of a heterogeneous reaction of N<sub>2</sub>O<sub>5</sub> to occur upon a molecular collision with an aerosol particle is described by the reactive uptake coefficient,  $\gamma$ . Laboratory and field studies have shown  $\gamma$  can be affected by aerosol particle chemical composition (Hanson and Ravishankara, 1991; Van Doren et al., 1991; Chang et al., 2011; Gaston et al., 2014). In a midlatitude flight campaign, Brown et al. (2007a) observed a strong dependence of  $\gamma$  on particle acidity and composition. Laboratory analysis has found that high concentrations of NO<sub>3</sub><sup>-</sup> in aerosol particles can hinder uptake of N<sub>2</sub>O<sub>5</sub> and suppress  $\gamma$  in a phenomena known as the “nitrate effect” (Mentel et al., 1999). Additionally, Reaction (R4b) was presented by Graedel and Keene (1995) as a sink of N<sub>2</sub>O<sub>5</sub> and the product, ClNO<sub>2</sub>, has been observed in the atmosphere (Osthoff et al., 2008; Thornton et al., 2010).

Bertram and Thornton (2009) found that trace amounts of Cl<sup>-</sup>, when the molar Cl<sup>-</sup>/NO<sub>3</sub><sup>-</sup> > 0.1, can negate the nitrate effect. They have characterized  $\gamma$ 's dependence on aerosol liquid water content, aqueous Cl<sup>-</sup> concentration, and aqueous NO<sub>3</sub><sup>-</sup> concentration in a parameterization for mixed organic and inorganic aerosol particles in the laboratory.

Other methods for parameterizing gamma have been developed. Chang et al. (2011) wrote an excellent review article on N<sub>2</sub>O<sub>5</sub> heterogeneous hydrolysis that describes various models for  $\gamma$ , comparison to ambient measurements, and size and chemical composition effects on  $\gamma$ . The nitrate effect and production of nitryl chloride are well documented by Chang et al. (2011) and cited references, as well as the effect of organic aerosol particle components, which generally is indicated to reduce  $\gamma$ , as described below. Evans and Jacob (2005) parameterized  $\gamma$  based upon aerosol particle type, and for some types  $\gamma$  was a function of temperature and relative humidity and performed global model simulations resulting in a global mean  $\gamma = 0.02$ , which is lower than Dentener and Crutzen (1993), but often larger than predicted by the Bertram and Thornton (2009) model. Anttila et al. (2006) described a resistor model for how organic coatings on inorganic core / organic shell aerosol particles could slow heterogeneous hydrolysis and Riemer et al. (2009) found that inclusion of these coatings slowed nitrate formation in a modeling study. Gaston et al. (2014) performed laboratory studies of the reduction of  $\gamma$  due to addition of organic to ammonium bisulfate aerosol particles. They found that low O : C ratios (atomic O : C ratio < 0.5) suppressed  $\gamma$ , while more highly oxygenated (O : C ratio > 0.8) species had little effect on  $\gamma$ . Ambient observations of  $\gamma$  (Bertram et al., 2009; Riedel et al., 2012; Ryder et al., 2014) or modeling of ambient levels of N<sub>2</sub>O<sub>5</sub> where  $\gamma$  is varied in the model to constrain its value (Brown et al., 2009; Wagner et al., 2013) have generally found that field measured  $\gamma$  values are lower by factors of 2 or more than the Bertram and Thornton (2009) parameterization. More recent studies have indicated that the inclusion of organic aerosol information and the particle mixing state improved the agreement between modeled and observed  $\gamma$ , but an  $\sim 2\times$  overprediction still exists in polluted air masses (Ryder et al., 2014). Only one study of  $\gamma$  during wintertime has been reported upon by Wagner et al. (2013). This study supports the nitrate effect, but unlike the other studies finds that the wintertime observed  $\gamma$  can be larger than that of the Bertram and Thornton (2009) model.

Because pollution is typically emitted at or near ground level, vertical gradients of reactive nitrogen species can easily form in nocturnal boundary layers, especially in cold and stable conditions. Observations of vertical distributions of NO<sub>3</sub> and N<sub>2</sub>O<sub>5</sub> demonstrated that nocturnal mixing ratios can vary widely over vertical scales of 10 m or less, implying that NO<sub>3</sub> and N<sub>2</sub>O<sub>5</sub> occupy distinctly different chemical regimes as a function of altitude (Brown et al., 2007b; Wagner et al., 2013). Aircraft observations of NO<sub>3</sub> and N<sub>2</sub>O<sub>5</sub> show that these species occur at larger concentrations and are

longer lived aloft than they are near the ground (Brown et al., 2007a). A modeling study by Geyer and Stutz (2004) found that slow upward transport of NO emitted near the ground, and the simultaneously occurring chemistry, controlled the vertical structure of the chemistry of NO<sub>x</sub>, NO<sub>3</sub>, and N<sub>2</sub>O<sub>5</sub>.

Such observations of vertical gradients of nocturnal nitrogen species may be due to competition between the removal of N<sub>2</sub>O<sub>5</sub> through Reaction (R4a) or (R4b) on aerosol particle surfaces aloft vs. deposition to the ground. Measurements of N<sub>2</sub>O<sub>5</sub> near Fairbanks in winter by our group found that sinks of N<sub>2</sub>O<sub>5</sub> (presumably heterogeneous chemistry) were an efficient mechanism for NO<sub>x</sub> removal near ground level (Ayers and Simpson, 2006). Apodaca et al. (2008) found that dry aerosol surface area was insufficient to explain the loss of N<sub>2</sub>O<sub>5</sub> observed, suggesting loss to other surfaces plays a key role. To characterize the loss to the snowpack, Huff et al. (2011) found the deposition velocity of N<sub>2</sub>O<sub>5</sub> to be  $0.59 \pm 0.47 \text{ cm s}^{-1}$  and that dry deposition represents at least 1/8 of the total chemical removal of N<sub>2</sub>O<sub>5</sub> near the ground. Theoretical studies of Kramm et al. (1995) calculated a somewhat higher N<sub>2</sub>O<sub>5</sub> deposition velocity that is towards the high end of our sensitivity studies. Understanding the magnitude of relative loss rates is essential for interpretation of N<sub>2</sub>O<sub>5</sub> measurements performed at ground level since air parcels near the ground surface will undergo loss both to aerosol particles and the snowpack.

Here we use a 1-D atmospheric chemistry model to address the fate of emitted NO<sub>x</sub> in high-latitude winter. A 1-D model allows for analysis of a theoretical atmospheric column composition versus height over time and comparison of loss processes, such as reaction of N<sub>2</sub>O<sub>5</sub> on aerosol particles versus the snowpack. Timescales for removal of NO<sub>x</sub> are analyzed and model sensitivities to parameters and constraints are examined.

## 2 Model description

### 2.1 General features

The meteorological and microphysical part of MISTRA (Microphysical STRatus) was originally a cloud-topped boundary layer model used for microphysical simulations of stratus clouds (Bott et al., 1996). MISTRA has been adapted as a marine and polar boundary layer model for studies of halogen chemistry (von Glasow et al., 2002; Piot and von Glasow, 2008) and includes gas-phase, liquid-phase, and heterogeneous chemistry, as well a microphysical module that explicitly calculates particle growth and treats interactions between radiation and particles. The full gas-phase reaction mechanism is available in the supplemental materials of Sommariva and von Glasow (2012), the aqueous mechanism is described in Pechtl et al. (2006), and photolysis rates are calculated online by the method of Landgraf and Crutzen (1998). Aerosol particles are initialized as the sum of three log-normal modes

based on the Jaenicke (1993) “urban” model and distributed into 70 bins by diameter. We note that these particles show a peak in the surface area distribution in the submicron range, where mass transport (diffusion) limitations to heterogeneous reactivity are less important than the reactive uptake coefficient. Calculations of kinetic rates are governed by IUPAC (International Union of Pure and Applied Chemistry) rate constants. Mixing is driven by turbulent heat exchange coefficient calculations. The model has 150 vertical layers from the bottom layer centered at a height of 5 m to the model top at 2000 m. The bottom 100 layers are spaced with a 10 m vertical resolution while the top 50 layers are spaced logarithmically. The model runs have a 10 s integration time with output every 15 min. For a more detailed description of the model see von Glasow et al. (2002).

MISTRA treats dry deposition of gases to the snowpack as an irreversible removal from the lowest atmospheric layer (5 m) to the snowpack below using a resistance model presented by Wesely (Wesely, 1989; Seinfeld and Pandis, 2006). The parameterization includes aerodynamic, quasi-laminar, and surface resistance and utilizes gas–aqueous equilibrium coefficients explicitly calculated for each species by MISTRA. Parameters for a mixed forest with wetland in a winter, sub-freezing environment were chosen (Wesely, 1989) and include resistance to deposition by buoyant convection and a lower ground “canopy” to simulate resistance to uptake by leaves, twigs, and other exposed surfaces. No resistance to deposition by large vegetation resistance is included. A dry deposition velocity of  $0.59 \text{ cm s}^{-1}$  is explicitly specified for N<sub>2</sub>O<sub>5</sub>, based on the field study by Huff et al. (2011), while all other dry deposition velocities are calculated using the parameterization by (Wesely, 1989). Significant dry deposition in the model occurs for species of interest: NO<sub>2</sub>, O<sub>3</sub>, N<sub>2</sub>O<sub>5</sub>, and HNO<sub>3</sub>. The dry deposition velocity for NO is calculated in MISTRA with the Wesely formulation but is unimportant, as found by Wesely and Hicks (2000).

The parameterization presented by Bertram and Thornton (2009) is used to calculate the accommodation coefficient,  $\alpha$ , which is used in Eq. (4) of von Glasow et al. (2002) to calculate the heterogeneous uptake rates of N<sub>2</sub>O<sub>5</sub> for each aerosol particle size bin in each model layer as a function of time. The difference in the resulting heterogeneous rate coefficient between this approach and using  $\gamma$  in the simple equation  $k = \gamma \bar{v} A / 4$  is less than 10% but it allows us to use a model-consistent way to calculate heterogeneous rate coefficients. Compared to the old approach as used in von Glasow et al. (2002), where  $\alpha = 0.1$ , the heterogeneous uptake rates of N<sub>2</sub>O<sub>5</sub> are now slower by a factor of up to 20. The Bertram and Thornton (2009) parameterization is dependent on aqueous NO<sub>3</sub><sup>-</sup> concentration, aqueous Cl<sup>-</sup> concentration, and aerosol particle liquid water content. This parameterization was chosen because it includes the nitrate effect and formation of nitryl chloride through chemical concentrations available in the model’s aerosol formulation. Although the organic component of aerosol particles is significant, we have

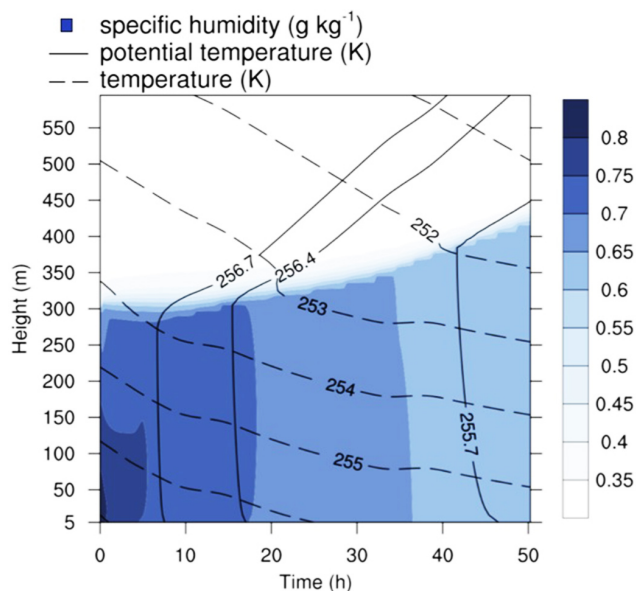


**Figure 2.** Modeled meteorological parameters include temperature (dashed contours), potential temperature (solid contours), and specific humidity (blue). The boundary layer height is initialized to be 300 m.

few observational details about the properties of this organic matter; for instance, we do not have the O : C ratio characterized, nor do we have any detailed information about the mixing state. Therefore, it was not possible to model the effect of the organic component of aerosol particles on  $\gamma$ . The only wintertime study of  $\gamma$  (Wagner et al., 2013) indicated that the Bertram and Thornton (2009) model was reasonably close to observations, sometimes underpredicting observed  $\gamma$  values. This cold-climate study's findings differ from the warmer-climate studies (e.g. Bertram et al., 2009; Riedel et al., 2012; Ryder et al., 2014), which found that organics poison N<sub>2</sub>O<sub>5</sub> heterogeneous reactivity.

To simulate a high-latitude atmospheric column moving in space, MISTRA is initialized with a clean Arctic air mass that then receives a pollution injection for 2 hours, corresponding to the contact time of an air parcel moving over Fairbanks at a speed of about 1 m s<sup>-1</sup>. Model runs begin at local midnight ( $t = 0$  h), with the pollution injection period beginning at  $t = 2$  h and ending at  $t = 4$  h. Injection occurs as a positive flux from the ground surface into the lowest model layer (5 m). No additional injection occurs after  $t = 4$  h and simulations continue until  $t = 50$  h for analysis 2 days “downwind” of the pollution source to focus on the fate of emitted NO<sub>x</sub>.

## 2.2 Observational constraints

Model runs did not attempt to simulate a specific day for comparison with observations, but rather typical conditions are presented to study the detailed chemical processes occurring under idealized conditions. The “base case” scenario is initialized as an average November day with a clear sky and snow covered ground with an albedo of 0.8. Photolysis rate calculations are performed online for 10 November at latitude 64.76° N, with a sunrise of 08:03 AKST and a sunset of 15:57 AKST. Both daytime and nighttime chemistry occur in the model. Photolysis rate calculations use a total column ozone of 401 Dobson units based the average of November 2009 observations over Fairbanks from the Total Ozone Mapping Spectrometer (TOMS, 2011). An initial temperature at ground level of 257 K (Fig. 2) is an observational average from 1929–2010 for November (ACRC, 2011). Relative humidity (RH) is initialized to 78 % in the mixed layer for the base case (Fig. 2) based on the average of November 2009 observations from the meteorological station located at the Fairbanks International Airport courtesy of the National Climate Data Center (NCDC, 2011).

Vertical mixing at high latitudes can become extremely hindered due to temperature inversions caused by strong radiative cooling from the ground surface at night. We know of no nocturnal vertical profiles of NO<sub>x</sub> species above Fairbanks in November, but a nocturnal in situ vertical profile of NO<sub>2</sub> was obtained in early April from the Arctic Research of the Composition of the Troposphere from Aircraft and Satellites (ARCTAS) campaign was available and also represents typical wintertime (inverted) conditions. Therefore, the ARCTAS NO<sub>2</sub> profile is used to constrain chemical vertical profiles in such conditions (ARCTAS, 2008). The flight originated at Fairbanks International Airport and took off at 02:23 AKST on 8 April 2008. NO<sub>2</sub> was detected from the surface up to an altitude of 300 m along a flight path to the southwest, downwind from downtown Fairbanks. The temperature profile obtained from the 8 April 2008 flight showed a surface inversion at an altitude of 50 m and a capping inversion at an altitude of 300 m. Vertical mixing in stable conditions often presents problems in model simulations (e.g., Anderson and Neff, 2008) and our simulations suffer from this as well. Attempts to simulate chemical profiles based on temperature profile observations did not yield results that agreed with the chemical profiles. Therefore, a mixed layer of 300 m is initialized using a dry-adiabatic lapse rate from the ground capped by a small isothermal layer (Fig. 2). The modeled vertical temperature profile allows for mixing of NO<sub>2</sub> to agree with the observed chemical vertical profile.

The chemical composition of the modeled atmospheric column at  $t = 0$  h represents an unpolluted Arctic air mass. Ambient ozone mixing ratios from Barrow, Alaska are 35 nmol mol<sup>-1</sup> on average from 2000–2010 in November, with peak abundances of 42 nmol mol<sup>-1</sup> (ESRL, 2011) and concentrations of polar aerosols found close to the surface

are generally very low (Seinfeld and Pandis, 2006). Therefore, the background chemical composition of the model is initialized as devoid of anthropogenic pollutants with an O<sub>3</sub> mixing ratio of 40 nmol mol<sup>-1</sup> and an aerosol particle loading of < 1 μg m<sup>-3</sup>.

The pollution injection during the “emission period” consists of NO, sulfur dioxide (SO<sub>2</sub>), ammonia (NH<sub>3</sub>), and aerosol particles containing organic matter, trace chloride (Cl<sup>-</sup>), and SO<sub>3</sub> that rapidly hydrolyzes to sulfuric acid (H<sub>2</sub>SO<sub>4</sub>) (Table 1). Sufficient NO emissions can “titrate” an air mass through Reactions (R1) and (R2), depleting O<sub>3</sub> and leading to an environment with excess NO, which is observed almost nightly during winter months in downtown Fairbanks (State of Alaska, 2008). The modeled NO flux is the smallest emission rate possible to titrate ozone to near zero through Reactions (R1) and (R2). This yields a modeled NO<sub>x</sub> mixing ratio of 58 nmol mol<sup>-1</sup> at the end of the pollution injection period (*t* = 4 h), which is within the first quartile (Q1) to third quartile (Q3) range of 31–103 nmol mol<sup>-1</sup> from observations in downtown Fairbanks (State of Alaska, 2008) and simultaneously brings O<sub>3</sub> down to 1 nmol mol<sup>-1</sup> at ground level. Emission of SO<sub>2</sub> is constrained by November 2008 average abundance observed in downtown Fairbanks (State of Alaska, 2008).

Ammonia and aerosol particle emissions are interrelated. Modeled aerosol particles are emitted as liquid particles containing organic material, highly oxidized sulfur species (e.g., SO<sub>3</sub> that rapidly hydrolyzes to sulfuric acid, H<sub>2</sub>SO<sub>4</sub>), and trace amounts of chloride and are constrained by PM<sub>2.5</sub> (aerosol particles with aerodynamic diameter < 2.5 μm) observations of particulate organic matter, sulfate, and chloride from downtown Fairbanks (ADEC, 2007) (Table 1). To obtain an appropriate aerosol number density and surface area, the number density of a standard tri-modal urban aerosol distribution (Jaenicke, 1993) is scaled to agree with the average PM<sub>2.5</sub> mass observation for November (ADEC, 2007). Sulfate (SO<sub>4</sub><sup>2-</sup>) concentrations from emitted highly oxidized sulfur species (e.g., SO<sub>3</sub> leading to H<sub>2</sub>SO<sub>4</sub>) are constrained on a percent-mass basis based on total PM<sub>2.5</sub>. The remaining observed aerosol particulate mass is primarily composed of organic carbon, elemental carbon, and heavy metals and is accounted for in the model using chemically inert dissolved organic matter.

Currently, there are no known ammonia observations in Fairbanks. Ammonia mixing ratios in remote areas can be < 50 pmol mol<sup>-1</sup> (Finlayson-Pitts and Pitts, 2000), so background NH<sub>3</sub> is initialized as 0.05 nmol mol<sup>-1</sup>. Biomass burning is a well documented source of ammonia emission (Yokelson et al., 1996, 1997; Akagi et al., 2011), suggesting combustion in woodstoves is a significant NH<sub>3</sub> source. Emission of ammonia is constrained based on ratios of CO and NO<sub>x</sub> emissions using Environmental Protection Agency (EPA) emission inventories and calculations based on previous studies. Carbon monoxide is produced from both automotive emissions and smoldering combustion in woodstoves.

The automotive fraction comes at least partially from cold starts and poor operation at cold temperatures. These cold-weather-related emissions have been targeted and the automotive CO source has decreased, with the last exceedance of National Ambient Air Quality standards for CO in 1999, implying that woodstove emissions are now a larger fraction of CO emissions. Studies of smoldering combustion composition by Yokelson et al. (1997) have shown ammonia is the primary nitrogen emission from a smoldering fire and estimate NH<sub>3</sub> emissions from burning wood to be 10.8 % of the CO emissions for white spruce harvested in Alaska. Recent southern California emissions of ammonia related to automotive operations have been found to be somewhat smaller at 3.3 ± 1.3 % mol NH<sub>3</sub>/mol CO (Nowak et al., 2012). However, emissions of CO in Fairbanks are related to cold weather not experienced in California, so the emissions ratio may be different. Therefore, we used the larger smoldering combustion emissions ratio as an estimate of combustion-related ammonia emissions. The EPA emissions inventory for Fairbanks in 2005 listed 1325 tons year<sup>-1</sup> (TPY) of CO (ADEC, 2008). Assuming all smoldering combustion emissions are produced in the winter, 6 months out of the year, this yields an estimate of 221 tons month<sup>-1</sup> (TPM) of CO. Assuming local fuel is consumed in woodstoves, the estimation using Yokelson et al. (1997) would yield 24 TPM NH<sub>3</sub>, currently not accounted for in the emissions inventory. For mobile sources, the emissions inventory reports 71 TPM NO<sub>x</sub> and 4 TPM NH<sub>3</sub> from annually occurring on-road, gasoline-powered sources. Calculations based on results from a study by Kean et al. (2000) suggest the magnitude of NH<sub>3</sub> emissions are 25 % that of NO<sub>x</sub> from automobiles due to use of three-way catalyst systems in gas-powered vehicles. By this estimate, on-road NH<sub>3</sub> from gas-powered vehicles is 18 TPM, an estimate 4.5 × higher than the NH<sub>3</sub> value listed in the inventory. Together, these estimates of NH<sub>3</sub> emissions from woodstoves and automotive sources make for 42 TPM NH<sub>3</sub>, which is 4.8 % of the total reported NO<sub>x</sub> emission of 872 TPM. Therefore, the ammonia flux during the emission period in the base case is constrained to be 4.8 % by mass of NO<sub>x</sub> emissions. Using the Nowak et al. (2012) California automotive ammonia / carbon monoxide emissions ratio and associating all wintertime CO with automotive emissions and no woodstove ammonia would lead to about 7 TPM automotive NH<sub>3</sub>, again significantly higher than in the inventory, but with lower total emissions than in the base case. We will address this uncertainty in ammonia emissions through sensitivity studies.

Another constraint on ammonia emissions comes from observed aerosol particle ammonium. Ammonia (NH<sub>3</sub>) readily protonates in acidic particles to form ammonium (NH<sub>4</sub><sup>+</sup>), increasing the pH. The molar ratio of NH<sub>4</sub><sup>+</sup>/SO<sub>4</sub><sup>2-</sup> in aerosol particles can be used to determine aerosol acidity, where a value above 2 indicates that all sulfuric acid has been neutralized. Data from downtown Fairbanks shows the first

**Table 1.** Emissions of pollutants in the base model case (at end of emissions,  $t = 4$  h) and observations from downtown Fairbanks. Q1–Q3 refers to first to third quartile range.

Emission Parameter	Base case 5 m, $t = 4$ h	Observed Q1–Q3 or average	Reference
NO <sub>x</sub> (nmol mol <sup>-1</sup> )	58	31–103	downtown Fairbanks, November 2008 (State of Alaska, 2008)
SO <sub>2</sub> (nmol mol <sup>-1</sup> )	12	8.8–20.6	downtown Fairbanks, November 2008 (State of Alaska, 2008)
NH <sub>3</sub> (nmol mol <sup>-1</sup> )	1.5	–	no known observations
PM <sub>2.5</sub> (μg m <sup>-3</sup> )	19	19	downtown Fairbanks, November 2008 average (ADEC, 2007)
PM <sub>2.5</sub> SO <sub>4</sub> <sup>2-</sup> (% mass)	0.18 %	0.18 %	downtown Fairbanks, November 2008 average (ADEC, 2007)
PM <sub>2.5</sub> Cl <sup>-</sup> (% mass)	0.4 %	0.5 %	downtown Fairbanks, November average (State of Alaska, 2011)
PM <sub>2.5</sub> NH <sub>4</sub> <sup>+</sup> /SO <sub>4</sub> <sup>2-</sup> (mol mol <sup>-1</sup> )	1.5	1.5–2.4	downtown Fairbanks, annual average (State of Alaska, 2011)

to third quartile range of molar NH<sub>4</sub><sup>+</sup>/SO<sub>4</sub><sup>2-</sup> to be 1.5–2.4 (State of Alaska, 2011). The modeled NH<sub>3</sub> emission from the ground, as explained above, is  $\sim 3\times$  the molar H<sub>2</sub>SO<sub>4</sub> emission, thus enough NH<sub>3</sub> is emitted to neutralize the sulfuric acid. Smaller emissions of ammonia become insufficient to neutralize sulfate aerosol particles, although sensitivity studies are carried out down to levels of ammonia emission  $5\times$  below the base case.

### 3 Results

#### 3.1 The urban pollution plume

The evolution of modeled primary emissions, destruction of ozone, and resulting products are shown in Figs. 3 and 4. All pollutants rapidly mix upon emission to 100 m at  $t = 4$  h, reaching 300 m at approximately  $t = 8$  h, then slowly diluting higher for the duration of the model run. The NO<sub>x</sub> vertical profile (Fig. 3a) shows a strong decrease with height at the end of the emission period due to ground-level emissions. Emitted NO<sub>x</sub> reaches 100 m altitude at the end of the emission period ( $t = 4$  h) and 300 m, the top of the initialized mixed layer, within 2 h after emissions cease ( $t = 6$  h).

Modeled total PM<sub>2.5</sub> (Fig. 3b) shows a vertical profile similar to NO<sub>x</sub> in the first 2 hours after the emission period ends ( $t = 6$  h) due to vertical dilution. No observations of aerosol number density and surface area are available for downtown Fairbanks for model evaluation. Modeled values at ground level at  $t = 4$  h reach a number density of  $2 \times 10^4$  cm<sup>-3</sup> and aerosol surface area density of 380 μm<sup>2</sup> cm<sup>-3</sup>. Modeled nitrate produced through secondary formation by Re-

action (R4a) and (R4b) in aerosol particles is 2 % of total PM<sub>2.5</sub> mass at  $t = 4$  h, compared to an average observed value of 4.4 % total PM<sub>2.5</sub> mass in November (ADEC, 2007). Background and emitted ammonia rapidly react with emitted acidic aerosol particles, forming particulate ammonium (Fig. 4f). Modeled ammonium in aerosol particles is 5 % by mass at  $t = 4$  h, and closely resembles ammonium observations comprising 6.4 % of total PM<sub>2.5</sub> mass (State of Alaska, 2011). Particulate ammonium formation leads to values of NH<sub>4</sub><sup>+</sup>/SO<sub>4</sub><sup>2-</sup> = 1.5 (Table 1) at the end of the emission period ( $t = 4$  h) through aerosol particle uptake and increases the molar ratio of NH<sub>4</sub><sup>+</sup>/SO<sub>4</sub><sup>2-</sup> to 2.1 one hour after the emission period ( $t = 5$  h). Column-integrated SO<sub>2</sub> remains constant in time, indicating that the model does not produce significant amounts of sulfate from oxidation of SO<sub>2</sub> in the base case, and the only loss mechanism of SO<sub>2</sub> from the atmosphere is dry deposition (not shown).

#### 3.2 Plume evolution in the base case

Previous field studies in Fairbanks were performed outside of the downtown area in order to observe un-titrated air masses that allow for formation of N<sub>2</sub>O<sub>5</sub>. Ayers and Simpson (2006) conducted measurements on the edge of the populated area of Fairbanks and observed both titrated and un-titrated air masses. Modeled dilution of NO<sub>x</sub> (Fig. 3a) agrees well with various field measurements in the greater Fairbanks area (Table 2), where abundances of NO<sub>x</sub> reduce with distance from downtown.

Background ozone (Fig. 4a) is depleted ( $< 2$  nmol mol<sup>-1</sup>) at ground level at  $t = 4$  h and is significantly reduced in the

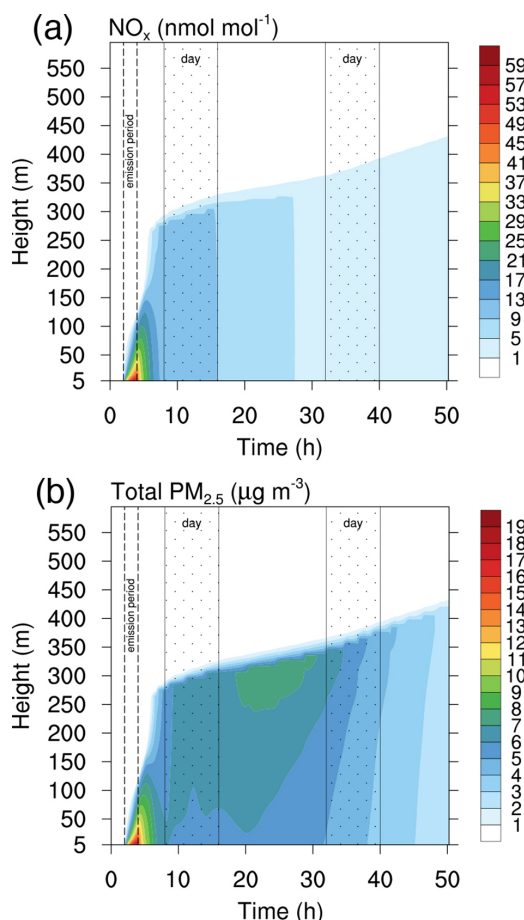


**Figure 3.** Modeled evolution of primary emission NO<sub>x</sub> and total PM<sub>2.5</sub> beginning at local midnight. Daytime regions are indicated by the dotted region and the emission period is indicated by the dashed lines. Emitted species dilute throughout the mixed layer. NO<sub>x</sub> undergoes chemical loss (a) while total PM<sub>2.5</sub> increases (b), primarily due to formation of particulate nitrate.

mixed layer due to titration of the air mass through Reactions (R1) and (R2). Ozone abundance returns to near-background levels approximately 4 hours after the pollution injection due to vertical mixing and photolysis of NO<sub>2</sub> in daylight hours.

Abundance of N<sub>2</sub>O<sub>5</sub> in the model (Fig. 4b) peaks aloft in the early morning of the first day ( $t = 9$  h) and in the middle of the second night (beginning  $t = 21$  h). The diurnal cycle of N<sub>2</sub>O<sub>5</sub> shows it is not produced during daylight hours, but peak levels can be maintained for about 1 day after NO emissions cease from the remaining NO<sub>x</sub> in the atmosphere. A reduction in the mixing ratio of N<sub>2</sub>O<sub>5</sub> near the ground occurs due to dry deposition to the snowpack. Modeled abundance of N<sub>2</sub>O<sub>5</sub> agrees well with observations by Ayers and Simpson (2006), but modeled N<sub>2</sub>O<sub>5</sub> near the ground is overestimated at longer distances (Table 2). This result is consistent with enhanced N<sub>2</sub>O<sub>5</sub> deposition to vegetation and enhanced turbulence due to surface vegetation and is discussed in Sect. 5.1.

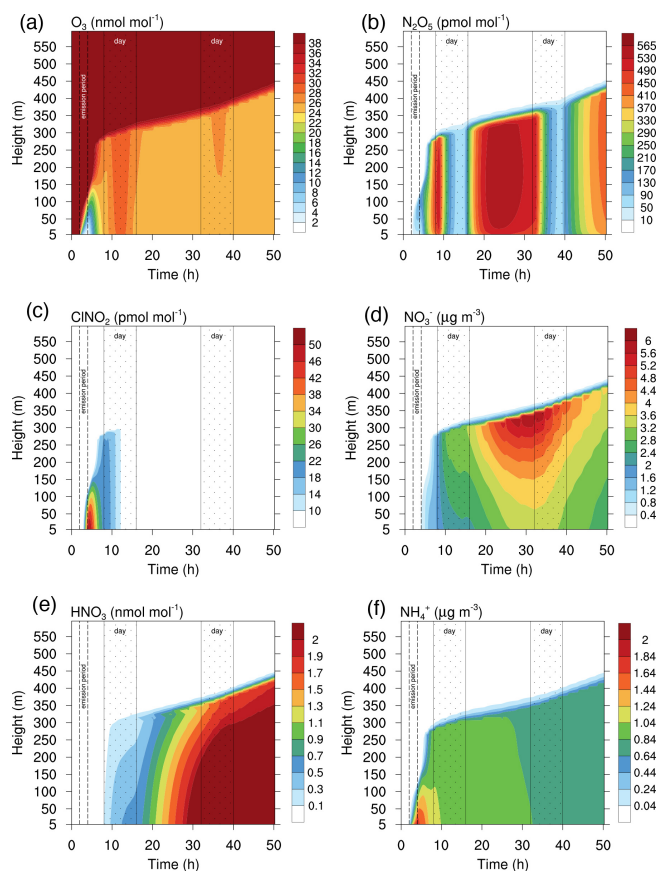


**Figure 4.** Contour plots of important gas-phase species. Modeled NO<sub>3</sub><sup>-</sup> and NH<sub>4</sub><sup>+</sup> are total aerosol mass density (sum of all aerosol particle sizes). Daytime regions are indicated by the dotted region and the emission period is indicated by the dashed lines.

Formation of ClNO<sub>2</sub> (Fig. 4c) occurs immediately upon formation of N<sub>2</sub>O<sub>5</sub> through Reaction (R4b) and removes trace Cl<sup>-</sup> in emitted aerosol particles (not shown) in less than 1 hour after emissions end ( $t = 5$  h). A reduction in N<sub>2</sub>O<sub>5</sub> mixing ratio below 50 m can be seen (Fig. 4b) from  $t = 4$  h to  $t = 5$  h that is due to ClNO<sub>2</sub> formation. Once formed, ClNO<sub>2</sub> dilutes through the mixed layer and abundances of  $\sim 20$  pmol mol<sup>-1</sup> throughout the mixed layer are lost through photolysis during the first day resulting in peak Cl radical concentrations of  $2.6 \times 10^3$  radicals cm<sup>-3</sup>. Formation of ClNO<sub>2</sub> is limited by aqueous Cl<sup>-</sup> concentrations in this simulation.

Particulate nitrate (Fig. 4d) is primarily formed through Reaction (R4a) and peaks  $\sim 24$  h after the emission period at the end of the second night, corresponding to reactive uptake of N<sub>2</sub>O<sub>5</sub> formed during the second night. Total nitrate (all aerosol particle sizes) peaks at a concentration of  $6.0$  µg m<sup>-3</sup> at an altitude of 325 m at  $t = 30$  h, where  $4.2$  µg m<sup>-3</sup> of the nitrate is in the PM<sub>2.5</sub> size fraction. Concentrations of nitrate at ground level reach a maximum of  $2.2$  µg m<sup>-3</sup> about 16 h after emission ends, showing a delay in secondary formation

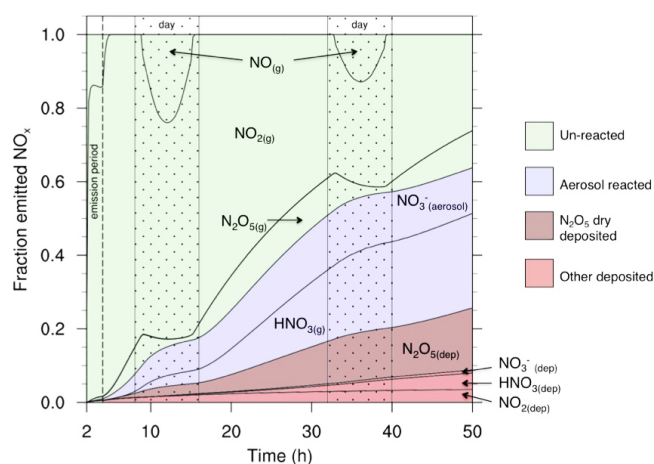


**Figure 5.** Speciation diagram of reactive nitrogen species showing column-integrated concentrations plus time integrated depositional loss as a function of time. Color categories correspond to Fig. 1.

of nitrate through the dark oxidation pathway. Gas-phase nitric acid (Fig. 4e) mixing ratio peaks within hours after the nitrate aerosol peaks and is outgassed by particles made acidic through Reaction (R4a). Larger aerosol particles are able to uptake greater amounts of  $\text{NO}_3^-$ . The peak number density of large aerosol particles ( $d > 2.5 \mu\text{m}$ ) occurs aloft, leading to increased  $\text{NO}_3^-$  aloft (Fig. 4d) and decreased abundance of gas-phase  $\text{HNO}_3$  aloft (Fig. 4e). The modeled  $\text{HNO}_3$  does not react readily with other species and will be ultimately removed through aerosol uptake upon mixing or deposition to the snowpack.

Formation of  $\text{NH}_4^+$  (Fig. 4f) occurs during the emission period and 1 hour immediately following emission due to aerosol particle uptake of  $\text{NH}_3$  and neutralization of emitted sulfuric acid aerosol particles. This process depletes background ammonia and emitted ammonia throughout the column (not shown) and forms ammonium sulfate  $[(\text{NH}_4)_2\text{SO}_4]$  or ammonium nitrate ( $\text{NH}_4\text{NO}_3$ ) in the particles. Once ammonium is formed in the aerosol particles they are well-mixed throughout the mixed layer and no losses from the atmosphere exist except aerosol particle deposition to the snowpack. Some additional ammonium is produced after the emission period due to entrainment from background ammonia above the mixed layer.

### 3.3 Fate of $\text{NO}_x$ in the base case

Nitrogen speciation is divided into four categories (Fig. 1) to characterize the state of emitted  $\text{NO}_x$  in time. Gas-phase nitrogen oxide species that have not yet undergone heterogeneous reaction on aerosol particles (R4a and R4b) are grouped into the term “un-reacted”, which is not meant to imply no reaction but simply no irreversible heterogeneous conversion to nitrate-type species. The un-reacted fraction includes  $\text{NO}_x$ ,  $\text{NO}_3^-$  (which is very small due to reactivity),  $\text{N}_2\text{O}_5$ , and

other reactive nitrogen species present in sub-pmol  $\text{mol}^{-1}$  range:  $\text{HONO}$  and  $\text{HNO}_4$ . The “aerosol-reacted” fraction includes any aqueous-phase  $\text{NO}_3^-$ ,  $\text{HNO}_3$  formed by nighttime chemistry then outgassed from acidic particles, and  $\text{ClONO}_2$  that remains suspended in the atmosphere. The “ $\text{N}_2\text{O}_5$  dry-deposited” fraction represents dry deposition of  $\text{N}_2\text{O}_5$  only. The “other deposited” fraction includes dry deposition of  $\text{NO}_2$  and  $\text{HNO}_3$  and deposition of  $\text{NO}_3^-$  aerosol. Reduced species  $\text{NH}_3$  and  $\text{NH}_4^+$  are not oxidized under simulation conditions and are not included in the speciation analysis.

Figure 5 presents a time series of speciation of emitted  $\text{NO}_x$ , depicted as the column-integrated fraction of each species out of the total emitted  $\text{NO}_x$ . Diurnal cycles discernible include the formation of  $\text{NO}$  and destruction of  $\text{N}_2\text{O}_5$  during the day. A vertical transect at any point in time depicts the current state of emitted  $\text{NO}_x$ . Most apparent is the trend of the un-reacted fraction decreasing with time. In the base case, only 36 % of un-reacted nitrogen remains in the atmosphere 2 days after the beginning of emissions ( $t = 50 \text{ h}$ ), with the remaining 63 % partitioned among the other categories (Fig. 5). The large fraction of gas-phase  $\text{HNO}_3$  (33 % at  $t = 50 \text{ h}$ ) is due to acidic aerosol conditions and represents a significant fate of emitted  $\text{NO}_x$ . Nighttime formation of  $\text{HNO}_3$  dominates gas-phase  $\text{HNO}_3$  production, but a small amount of  $\text{HNO}_3$  production can be seen in the afternoon periods due to the daytime oxidation pathway. Dry deposition of  $\text{HNO}_3$  through the aerosol-reacted pathway is the fate of 5 % of the total emitted  $\text{NO}$  after 2 days, but is less than the  $\text{N}_2\text{O}_5$  dry-deposited fraction of 17 %. Dry deposition of  $\text{N}_2\text{O}_5$  makes up a discernable fraction 2 hours after the emission period ends while  $\text{NO}_3^-$  aerosol deposition and  $\text{HNO}_3$  dry deposition does not build until 16 h after the emission period ends. A slight increase in dry deposition occurs during the day due to increased turbulent mixing. Other reactive nitrogen species such as  $\text{HONO}$ ,  $\text{HNO}_4$ , and  $\text{N}_2\text{O}_4$  are included with the  $\text{NO}_2$  fraction and make up an insignificant portion ( $< 1 \%$ ).

## 4 Sensitivity of the fate of $\text{NO}_x$ to model parameters

Experiments were performed to analyze the sensitivity of the fate of  $\text{NO}_x$  to model constraints by modifying parameters over ranges based on realistic conditions. These experiments are presented as demonstrations of model performance as well as representations of the base case under changing scenarios. The sensitivities found to be most significant are described below and are depicted in Fig. 6a–h. Analysis of each experiment is conducted by relative comparison of total nitrogen fractions in each speciation category 2 days after the emission period ends ( $t = 50 \text{ h}$ ).

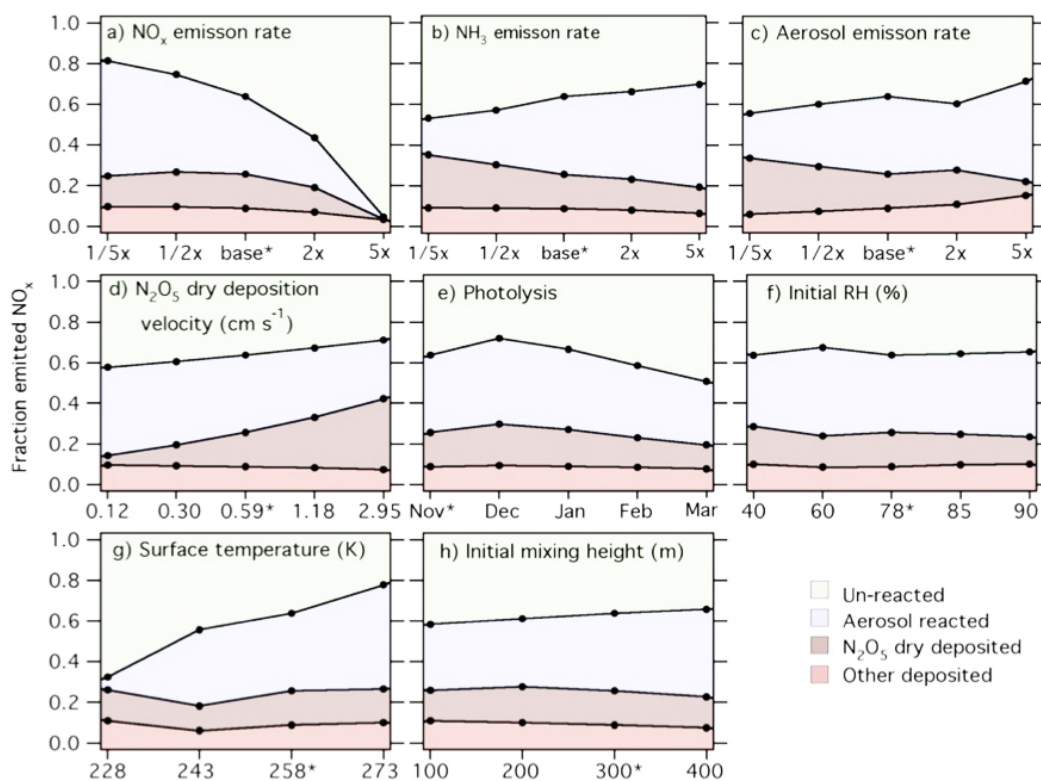


**Figure 6.** Sensitivity of the fate of emitted NO<sub>x</sub> to model parameters was investigated by variations of constraints on the base case. Shown are speciation fractions of total column nitrogen emitted as NO<sub>x</sub> at  $t = 50$  h, corresponding to 2 days after the emission period begins. Base case runs are marked by an asterisk (\*).

#### 4.1 NO emission rate

Increased flux of NO during the emission period leads to increased NO<sub>x</sub> abundance, most intensely near the ground. Increased mixing ratio of NO depletes O<sub>3</sub> in the mixed layer, slowing Reactions (R1) and (R2) and N<sub>2</sub>O<sub>5</sub> formation. This slowing of N<sub>2</sub>O<sub>5</sub> formation causes the un-reacted fraction to remain dominant. The 5×-NO-case represents a strongly titrated air mass. In this case, modeled NO<sub>x</sub> reaches 300 nmol mol<sup>-1</sup> at  $t = 4$  h, within the range of downtown observations (Table 1), leaving excess NO and depleted ozone at night throughout the mixed layer for the entire duration of the run, suppressing N<sub>2</sub>O<sub>5</sub> formation and slowing nocturnal oxidation of NO<sub>x</sub>. Alternatively, under a lower NO emission rate, NO<sub>x</sub> is efficiently removed through the dark oxidation pathway, with preference for the aerosol-reacted fraction.

#### 4.2 NH<sub>3</sub> emission rate

Increased emissions of NH<sub>3</sub> lead to greater amounts of NO<sub>3</sub><sup>-</sup> retention in the particulate phase, giving increased particulate surface area and thus a greater aerosol-reacted fraction. This result was somewhat surprising because we expected that the increased nitrate effect from enhanced NO<sub>3</sub><sup>-</sup> retention would

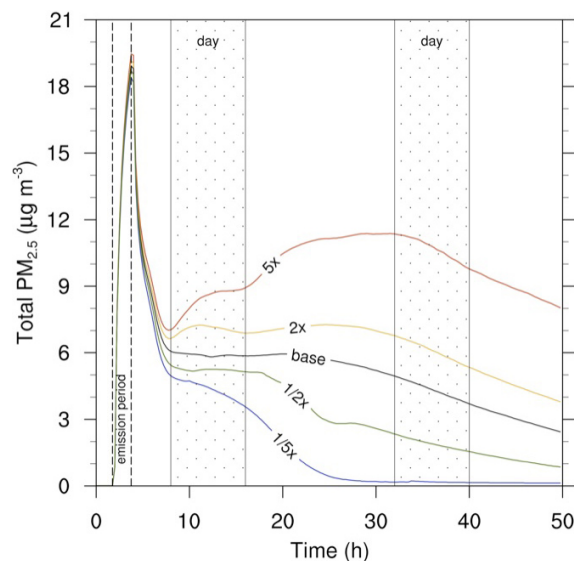


**Figure 7.** Secondary formation of ammonium nitrate begins at  $t = 8$  h and is controlled in magnitude by NH<sub>3</sub> abundance. The delay of ammonium nitrate formation after emissions end is due to the slowness of nocturnal oxidation caused by ozone titration present during the first night. Pictured above is total PM<sub>2.5</sub> for the lowest model layer (5 m) for each NH<sub>3</sub> sensitivity experiment.

decrease the reactive uptake coefficient, according to the parameterization by Bertram and Thornton (2009), and reduce the aerosol particle reactivity. However, the heterogeneous uptake rate is not only determined by reactive uptake limitations, and in this case the larger available reactive surface area outweighs the reduction in the reactive uptake coefficient due to the nitrate effect. This sensitivity is discussed further in Sect. 5.3.

### 4.3 Aerosol emission rate

In general, increased aerosol flux from the surface leads to greater aerosol particle number density, surface area, and mass density of sulfate particles. Primary sulfate emissions do not leave the particles and thus lead to increased total aerosol particle mass. The increase in aerosol particle surface area allows for more surface reactivity and increases the aerosol-reacted fraction and aerosol particle deposition in the other deposited fraction over the  $1/5\times-5\times$  factor sensitivity experiments. Additionally, the N<sub>2</sub>O<sub>5</sub> dry-deposited fraction is decreased due to the enhanced aerosol uptake. The decrease of the aerosol-reacted fraction in the  $2\times$  experiment requires further examination, but is likely a feedback based on NO<sub>x</sub> emission and time of analysis ( $t = 50$  h).

As discussed in the introduction, the reactive uptake coefficient calculation model (Bertram and Thornton, 2009) may overestimate reactive uptake rates, particularly in the case where organic components coats particulate surfaces. Because the rate of N<sub>2</sub>O<sub>5</sub> heterogeneous hydrolysis is dependent upon both the aerosol particle surface area and the reactive uptake coefficient, the effect of increasing the latter is likely to be similar to increased aerosol particulate emissions. Therefore, we would expect that if the actual reactive uptake coefficient is lower than calculated by Bertram and Thornton (2009), as has been observed in the presence of organic coatings (Bertram et al., 2009; Riedel et al., 2012; Ryder et al., 2014), the aerosol-reacted fraction would decrease. Alternatively, if the actual  $\gamma$  is larger than modeled, as has been observed at times during the wintertime study of Wagner et al. (2013), the aerosol-reacted fraction would be expected to increase.

### 4.4 N<sub>2</sub>O<sub>5</sub> dry deposition velocity

The empirical value of dry deposition velocity of N<sub>2</sub>O<sub>5</sub> was found to be between 0.12 and 1.06 cm s<sup>-1</sup> (Huff et al., 2011) and covered by the range of the  $1/5\times-2\times$  sensitivity experiments. The total fraction of N<sub>2</sub>O<sub>5</sub> dry deposited varies from 5 % to 25 % over this range. Increases in the dry deposition velocity of N<sub>2</sub>O<sub>5</sub> lead to an increase in the N<sub>2</sub>O<sub>5</sub> dry-deposited fraction, a corresponding decrease in all other fractions, and a reduction of N<sub>2</sub>O<sub>5</sub> mixing ratio at ground level, near the snowpack.

### 4.5 Photolysis

In this experiment, photolysis calculations are carried out for 10 November, 21 December, 22 January, 21 February, and 20 March. The lowest photolysis rate (21 December) corresponds to the smallest un-reacted fraction. Under the weakest photolysis conditions, N<sub>2</sub>O<sub>5</sub> is present at all hours and reaches a minimum value of 200 pmol mol<sup>-1</sup> throughout the mixed layer during the day. This N<sub>2</sub>O<sub>5</sub> abundance allows for nitrate formation via the dark oxidation pathway through Reaction (R3) for 24 h per day. Increased photolysis and longer periods of daylight (20 March) leads to an increased un-reacted fraction due to limitation of Reaction (R3) during the shorter nights and weak daytime oxidation of NO<sub>x</sub>. Monthly average temperatures in winter in Fairbanks are very similar due to large temperature fluctuations over a monthly time period, and each month is likely to have days near the base case temperature of 258 K. For a sensitivity experiment with respect to temperature, see (Sect. 4.7).

### 4.6 Initial RH

This experiment modifies the initial RH in the mixed layer. Increases in RH lead to increases in aerosol surface area from water vapor to particle equilibrium, which is calculated by the model. Most substantial in a relatively dry mixed layer, a 20 % increase in RH from 40 % to 60 % increase the aerosol-reacted fraction by 9 %.

### 4.7 Surface temperature

For this experiment, temperature at the bottom layer of the atmosphere ranges from 228 K to 273 K, which could occur on any given day during the months of November to March. Decreasing temperatures produce a significantly greater un-reacted fraction due to kinetic limitation of reactions.

### 4.8 Initial mixing height

The mixed layer in the model gradually rises in time (Fig. 2) due to mixing from above. Due to the time needed to mix air throughout the 300 m mixed layer ( $\sim 6$  h), the height of the mixed layer is nearly constant at 100 m at the end of the emission period for all runs (100–400 m) and therefore does not affect constrained mixing ratios of emissions. Thus, this experiment shows variation of the dilution downwind of the emission source due to a variable mixed layer height. Increases in the height of the mixed layer decrease both N<sub>2</sub>O<sub>5</sub> dry deposited and other deposited fractions while increasing the amount of aerosol-reacted fraction retained in the atmosphere due to less contact with the snowpack surface.

### 4.9 Chloride concentration (not shown)

In this experiment, the aqueous concentration of emitted chloride in aerosol particles varies from zero– $5\times$  base to

determine the effect on NO<sub>x</sub>. This range leads to a particulate chloride concentrations of 0.00–0.56 μg m<sup>-3</sup> at  $t = 4$  h near the ground. These trace amounts of Cl<sup>-</sup> present in the particles slightly reduce the aerosol-reacted fraction, while the aerosol-reacted fraction increases by 3 % when no Cl<sup>-</sup> is included. This weak sensitivity of the fate of NO<sub>x</sub> to particulate chloride is likely due to analysis occurring 2 days after emission. Analysis undertaken less than 8 hours after emissions end yields a larger sensitivity to Cl<sup>-</sup> due to the presence of ClNO<sub>2</sub> in the aerosol-reacted fraction. Significant reductions in N<sub>2</sub>O<sub>5</sub> mixing ratio and nitrate production are seen (Fig. 4b) in the first hours after emission ends due to the production of ClNO<sub>2</sub>. Therefore, aerosol chloride concentrations may have a much greater impact on the local scale.

#### 4.10 Time of day (not shown)

The start of the emission period was varied to analyze the effect of photolysis on the fresh or aged plume. With respect to local impacts (under 8 h), the time of day has a significant effect on column composition by hindering or allowing the dark oxidation pathway to occur immediately after emission. Therefore, the time of day of NO<sub>x</sub> emission is found to have a significant effect on N<sub>2</sub>O<sub>5</sub> deposition on a local scale, where NO<sub>x</sub> emissions in daylight are likely to travel farther from the source before undergoing oxidation, and NO<sub>x</sub> emissions at night will enhance local deposition. By  $t = 50$  h, however, the plumes are exposed to approximately equal amounts of sunlight and there is no significant effect on the fate of NO<sub>x</sub>.

#### 4.11 SO<sub>2</sub> emission (not shown)

Weak photolysis conditions in the base case do not allow for significant secondary formation of sulfate by SO<sub>2</sub> oxidation by the OH radical. Therefore, SO<sub>2</sub> is virtually inert in these simulations and does not affect the fate of NO<sub>x</sub>.

#### 4.12 Deposition to canopy (not shown)

An additional experiment was performed to include the “upper canopy” term (see Seinfeld and Pandis, 2006) of mixed forest in the dry deposition parameterization to simulate deposition to trees. The addition of an upper canopy parameter in the dry deposition equation leads to increases of dry deposition velocity of 10 % for HNO<sub>3</sub>, 16 % for NO<sub>3</sub>, and by 1 order of magnitude for NO<sub>2</sub>. The explicitly set value for dry deposition velocity of N<sub>2</sub>O<sub>5</sub> is scaled up by 10 % for this experiment, based on the result for HNO<sub>3</sub>. Including the upper canopy results in a 4 % increase in the other deposited fraction, primarily due to increased NO<sub>2</sub> deposition, and a < 1 % increase in the N<sub>2</sub>O<sub>5</sub> dry-deposited fraction. In this 1-D model, the addition of deposition to the upper canopy of trees has an insignificant effect on the fate of NO<sub>x</sub>. However, air transport over horizontally varying trees causes mixing of surface and near-surface layers that may

enhance deposition in a way we cannot model in this 1-D simulation. This point is discussed below.

## 5 Discussion

### 5.1 Local effects vs. long-range transport

Results from the base case speciation analysis (Fig. 5) have implications for local and long-range deposition effects. Dry deposition of N<sub>2</sub>O<sub>5</sub> begins immediately upon formation of N<sub>2</sub>O<sub>5</sub> and dominates the nitrogen flux to the snowpack during the night. Snowpack deposition of aerosol nitrate and gas-phase HNO<sub>3</sub> does not occur in significant amounts until 16 h after emissions have ended. This indicates dry deposition of N<sub>2</sub>O<sub>5</sub> dominates nitrogen deposition to the snowpack on a local scale, while particulate nitrate deposition is minimal. Alternatively, particulate nitrate can remain suspended in the local atmosphere, undergo long-range transport, be diluted in transit, and removed by a precipitation event.

Observations of both titrated and un-titrated air masses in studies such as Ayers and Simpson (2006) indicate a wide variability of the oxidation capacity of the mixed layer. Sensitivity experiments presented here have shown NO emissions in the absence of photolysis can transform the lower atmosphere from an oxidizing environment rich in ozone to a reduced environment with no oxidation capacity. Some values of NO<sub>x</sub> observed in downtown Fairbanks are even greater than the modeled 5×-NO<sub>x</sub> experiment (Fig. 6a) in which ozone was titrated in the mixed layer for 2 days. In reality, horizontal mixing may reduce the timescale of titration as background ozone is mixed in, but ozone reduction may linger for well over 24 h downwind. Ozone titration is likely to be enhanced under stable meteorological conditions.

The photolysis experiment (Fig. 6e) has implications for environments at higher latitudes than Fairbanks, which is located at 64.76° N. The month of December, with the weakest photolysis and longest periods of darkness, shows the smallest un-reacted fraction. Dry deposition of N<sub>2</sub>O<sub>5</sub> and aerosol-reacted fractions are enhanced by extended darkness. Locations north of the Arctic Circle (66.56° N) will have days on which no photolysis will occur and N<sub>2</sub>O<sub>5</sub> formation occurs continuously, allowing the dark oxidation pathway of NO<sub>x</sub> to be active 24 h per day. Under total darkness conditions, local deposition of N<sub>2</sub>O<sub>5</sub> is likely to be enhanced.

The drastic dependence of the fate of NO<sub>x</sub> on temperature (Fig. 6g) shows that ambient temperatures are the most important naturally occurring factor controlling the chemistry of the nocturnal NO<sub>x</sub> plume. The primary reason for the increased un-reacted fraction is that the formation rate of NO<sub>3</sub> slows at colder temperatures, leaving a larger fraction of NO<sub>x</sub> un-reacted at the  $t = 50$  h analysis time. Interestingly, dry deposition rates of N<sub>2</sub>O<sub>5</sub> remain fairly constant over this temperature range. The range of temperatures studied are not uncommon in Fairbanks for the months of November to March.

For temperatures lower than 228 K and stable meteorological conditions, NO<sub>x</sub> may be near the snowpack for extended periods of time, possibly enhancing dry deposition.

## 5.2 Vertically varying chemistry

Modeled vertical profiles of N<sub>2</sub>O<sub>5</sub> have implications for interpreting field measurements. Modeled N<sub>2</sub>O<sub>5</sub> mixing ratio at 105 m one hour immediately following the emission period ( $t = 5$  h) is over 2× greater than at the surface and consistently 10–15 % greater for the duration of the model run. This suggests that observations carried out near the snowpack may yield abundances of N<sub>2</sub>O<sub>5</sub> significantly lower than those aloft. More importantly, positive vertical gradients of N<sub>2</sub>O<sub>5</sub> reaffirm the result found by Huff et al. (2011) that dry deposition is a significant loss mechanism of N<sub>2</sub>O<sub>5</sub> near the snowpack.

Additionally, loss of N<sub>2</sub>O<sub>5</sub> near the ground may be underestimated. Modeled values of N<sub>2</sub>O<sub>5</sub> aloft in the first hour after emissions end ( $t = 5$  h) are in good agreement with measurements performed 80 m above the valley floor (Table 2). This suggests the model properly captures loss of N<sub>2</sub>O<sub>5</sub> aloft on short timescales (a few hours). At longer distances and near the ground, the model predicts ~4× observed abundances of N<sub>2</sub>O<sub>5</sub> (Table 2). The measured dry deposition velocity of N<sub>2</sub>O<sub>5</sub> used to constrain the model was based on aerodynamic methods and measured above a treeless, flat snowpack. Under this constraint, the model assumes a flat ground surface for the entire model run, whereas Fairbanks is surrounded by densely wooded terrain, which enhances turbulence due to roughness. This turbulence is expected to enhance deposition of N<sub>2</sub>O<sub>5</sub> and thus reduce observed N<sub>2</sub>O<sub>5</sub> when compared to modeled values, which is a treeless environment free of mechanical turbulence.

The effect of enhanced turbulence near the ground would increase air parcel transport to the ground surface, with a result similar to that of a sensitivity experiment with enhanced dry deposition velocity of N<sub>2</sub>O<sub>5</sub>. The model scenario with an enhanced value of 2.95 cm s<sup>-1</sup> (Fig. 6d) still predicts N<sub>2</sub>O<sub>5</sub> abundance near the ground ~2× greater than observed values. This method is not the correct way to address enhanced deposition because deposition velocity is increased rather than air parcel contact with the snowpack. It does, however, suggest that deposition of N<sub>2</sub>O<sub>5</sub> may be significantly underestimated in the treeless model scenario. Modeling enhanced deposition due to mechanical turbulence induced by a 3-D object such as tree cover is a limitation of the 1-D model. Airborne observations of N<sub>2</sub>O<sub>5</sub> aloft, away from Fairbanks, would verify if the model properly captures loss of N<sub>2</sub>O<sub>5</sub> away from the ground and would verify that loss to ground surface is underestimated. Such observations are necessary to fully understand the vertical and spatial distribution of the nocturnal nitrogen plume.

## 5.3 Ammonium nitrate formation

Downtown Fairbanks lies in a US Environmental Protection Agency non-attainment area for PM<sub>2.5</sub> (ADEC, 2008). A common concern in reducing total PM<sub>2.5</sub> lies in a non-linearity present in aerosols containing ammonium, nitrate, and sulfate. When excess ammonia is available (molar ratio of NH<sub>4</sub><sup>+</sup>/SO<sub>4</sub><sup>2-</sup> > 2), reductions in particulate sulfate may be replaced by particulate nitrate, leading to an increase of ammonium nitrate in the aerosol particles (Seinfeld and Pandis, 2006, p. 483). Modeled particulate nitrate concentrations in the polluted area ( $t = 4$  h) are < 0.5 μg m<sup>-3</sup> and agree with observations (ADEC, 2007), but concentrations of > 2 μg m<sup>-3</sup> NO<sub>3</sub><sup>-</sup> are modeled within 6 hours after emissions end. These results suggest that secondary particulate nitrate formation due to NO<sub>x</sub> oxidation within Fairbanks urban core is not a major contributor to PM<sub>2.5</sub> non-attainment because titration of O<sub>3</sub> slows N<sub>2</sub>O<sub>5</sub> formation and thus formation of NO<sub>3</sub><sup>-</sup> and HNO<sub>3</sub>. Enhanced secondary formation of particulate nitrate, however, may have implications further downwind of the polluted area.

In the NH<sub>3</sub> emission rate sensitivity experiment (Fig. 6b), the aerosol-reacted fraction increases with increased ammonia emissions. This effect can be seen in total PM<sub>2.5</sub> concentrations near the ground (Fig. 7) beginning 2 hours after the end of emissions due to the formation of ammonium nitrate (NH<sub>4</sub>NO<sub>3</sub>). During the emission period, primary emissions of fully oxidized sulfur leading to H<sub>2</sub>SO<sub>4</sub> and organic matter dominate total mass and are similar for each experiment. During the emission period and for ~2 h afterward, NH<sub>4</sub>NO<sub>3</sub> concentrations are zero and NH<sub>4</sub><sup>+</sup>/SO<sub>4</sub><sup>2-</sup> < 2 in the particle and sulfuric acid is not fully neutralized. Base case emissions of NH<sub>3</sub> are sufficient to bring the molar ratio of NH<sub>4</sub><sup>+</sup>/SO<sub>4</sub><sup>2-</sup> at the surface to 1.5 at  $t = 4$  h, which gradually increases to 2.1 at  $t = 5$  h. Values of NH<sub>4</sub><sup>+</sup>/SO<sub>4</sub><sup>2-</sup> > 2 are possible as NO<sub>3</sub><sup>-</sup> is formed and available to react with NH<sub>4</sub><sup>+</sup> to form NH<sub>4</sub>NO<sub>3</sub> (Seinfeld and Pandis, 2006, p. 479). Increases in the NH<sub>3</sub> flux bring the NH<sub>4</sub><sup>+</sup>/SO<sub>4</sub><sup>2-</sup> ratio at the end of the emission period ( $t = 4$  h) to 1.9 for the 5× NH<sub>3</sub> run. Divergence of total PM<sub>2.5</sub> mass at  $t = 8$  h (Fig. 7) between the sensitivity studies is controlled by NH<sub>3</sub> emission and subsequent formation of NH<sub>4</sub>NO<sub>3</sub>. In this manner, secondary formation of nitrate particles is controlled in magnitude by ammonia flux and the rate of nocturnal NO<sub>x</sub> oxidation, which is strongly affected by ozone titration. In all cases, secondary aerosol mass continues to form during the first day while N<sub>2</sub>O<sub>5</sub> is still present from nighttime formation (Fig. 7). Dry deposition of ammonia gas competes with uptake of ammonia by aerosol particles and neutralization of particulate acidity, so in cases where vertical mixing is hindered, deposition of ammonia may also limit the uptake to aerosol particles.

The slow timescale of NH<sub>4</sub><sup>+</sup> uptake by aerosol forming NH<sub>4</sub>NO<sub>3</sub> makes it impossible to infer NH<sub>3</sub> abundances

**Table 2.** Field observations of NO<sub>x</sub> from downtown Fairbanks, University of Alaska Fairbanks (UAF), and the Quist Farm as well as related model results. A wind speed of 1 m s<sup>-1</sup> and distance from downtown was used to calculate corresponding model time. Observations at UAF were performed at an elevation 80 m above the valley floor (<sup>1</sup>) and compared to modeled values in layer centered at 75 m (<sup>2</sup>).

	Downtown	UAF	Quist Farm
Distance from downtown (km, direction)	0	5, WNW	20, WSW
Corresponding model time (h)	4	5	8
Modeled NO <sub>x</sub> (nmol mol <sup>-1</sup> )	58	24 <sup>2</sup>	12
Observed NO <sub>x</sub> range (nmol mol <sup>-1</sup> )	1–390	0–100 <sup>1</sup>	0–15
Modeled N <sub>2</sub> O <sub>5</sub> (pmol mol <sup>-1</sup> )	38	182 <sup>2</sup>	412
Observed N <sub>2</sub> O <sub>5</sub> range (pmol mol <sup>-1</sup> )	–	0–250 <sup>1</sup>	0–80
Reference	State of Alaska (2008)	Ayers and Simpson (2006)	Huff et al. (2011)

downtown based on NH<sub>4</sub><sup>+</sup> measurements. Due to the slow timescale of nitric acid and particle nitrate formation, a decrease in primary sulfate emissions should reduce total PM<sub>2.5</sub> and not be replaced by an increase in particulate nitrate in the downtown area. However, this NO<sub>x</sub> is later oxidized to HNO<sub>3</sub> and particulate NO<sub>3</sub><sup>-</sup>, which later reacts with NH<sub>3</sub> forming NH<sub>4</sub>NO<sub>3</sub> that could result in soil fertilization downwind of Fairbanks.

Constrained by emissions inventories and calculations, NH<sub>3</sub> emissions yielded a value of 0.96 μg m<sup>-3</sup> NH<sub>4</sub><sup>+</sup> and 1.6 nmol mol<sup>-1</sup> excess NH<sub>3</sub> near the ground at the end of the emission period ( $t = 4$  h). In order to achieve the measured November average of 0.97 μg m<sup>-3</sup> NH<sub>4</sub><sup>+</sup> (State of Alaska, 2011) through aerosol uptake, we estimate that a minimum of 1.2 nmol mol<sup>-1</sup> NH<sub>3</sub> needs to be available for uptake into aerosol particles. The base-case-emitted NH<sub>3</sub> was sufficient to reach NH<sub>4</sub><sup>+</sup> observations and yield excess NH<sub>3</sub>. We believe automotive and woodsmoke sources of NH<sub>3</sub> are sufficient to account for the measured NH<sub>4</sub><sup>+</sup>/SO<sub>4</sub><sup>2-</sup> ratio. Results of sensitivity experiments have shown NH<sub>3</sub> could be greater than modeled in the base case with no indication present in NH<sub>4</sub><sup>+</sup> observations downtown due to slow NH<sub>4</sub>NO<sub>3</sub> formation caused by titration. However, if there are larger than the base case ammonia emissions, significantly enhanced formation of NH<sub>4</sub>NO<sub>3</sub> is modeled outside of the primarily polluted area. Therefore, observations of NH<sub>3</sub> emissions would be highly valuable for understanding Fairbanks air quality and possible downwind ecosystem impacts through ammonium nitrate deposition.

The origin and chemistry of sulfate aerosol in Fairbanks winter is currently unknown. The emissions used in this simulation, constrained by gas-phase SO<sub>2</sub> and PM<sub>2.5</sub> SO<sub>4</sub><sup>2-</sup> observations, estimate column-integrated total sulfur is in the form of 93 % SO<sub>2</sub> and 7 % fully oxidized sulfur (e.g., SO<sub>3</sub>) that rapidly reacts to form SO<sub>4</sub><sup>2-</sup>. A value of 7 % is likely

too high to be purely primary sulfate emission, but the modeled base case scenario produces no secondary sulfate from SO<sub>2</sub>, which would be expected in an atmosphere with weak OH photochemistry and reduced oxidants (due to titration of ozone). Sulfur oxidation catalysis by transition metals has been presented as a sulfate formation mechanism (Brandt and van Eldik, 1995; Hoffman and Boyce, 1983) and could be a significant secondary SO<sub>4</sub><sup>2-</sup> source during winter. If the formation of SO<sub>4</sub><sup>2-</sup> by metal catalysis is fast, the sulfate could appear like true primary emissions, as we have modeled them in this study. The fate of NO<sub>x</sub> emissions is found to be insensitive to SO<sub>2</sub>, but this may not have been the case if secondary sulfate was formed by pathways alternative to photochemistry. Additional study would be useful for understanding the sulfate chemistry in Fairbanks and identifying possible remedies for PM<sub>2.5</sub> non-attainment.

#### 5.4 Model limitations

The simulations in this experiment presented for analysis of the fate of anthropogenic NO<sub>x</sub> pollution in a high-latitude environment are not without a few limitations. The meteorological conditions in the model were chosen such that cloud formation is avoided, primarily because microphysical and chemical feedbacks would hinder the main focus of this study, which was the fate of emitted NO<sub>x</sub> in a high-latitude winter environment. Clear skies dominate synoptic conditions in the greater Fairbanks area in the winter months, supporting that the base case simulation is not weakened by the absence of clouds. Observations by Sommariva et al. (2009) found that N<sub>2</sub>O<sub>5</sub> removal by fog droplets was dominant when fog was present. Cloud formation would likely lead to dominance of N<sub>2</sub>O<sub>5</sub> uptake aloft in large cloud particles, leading to less gas-phase HNO<sub>3</sub> and more nitrate aloft which could undergo long-range transport. Cloud formation would also affect photolysis rates in model layers below the clouds.

The temperature profile used to initialize the model was not taken from an individual measured profile but rather an idealized case because this idealized case better replicated the ARCTAS NO<sub>2</sub> profile. This model deficiency is a common problem for numerical models of the stable boundary layer (see discussion in Anderson and Neff, 2008). The NO<sub>2</sub> detected by the ARCTAS aircraft at 300 m was 14 km from downtown Fairbanks (ARCTAS, 2008). Assuming column motion of about 1 m s<sup>-1</sup>, 14 km would correspond to the modeled NO<sub>x</sub> profile at  $t = 8$  h, which shows vertical dilution to  $\sim 290$  m. The modeled temperature profile of the base case is applicable for conditions with relatively high mixed layers and weak inversions, which are common in the “shoulder” months of October, November, March and April. Mixing due to the modeled temperature gradient is suitable for this study; however, mixing forced by eddy-diffusivity has been performed to match observed vertical profiles (Geyer and Stutz, 2004) and may be more appropriate for thermally inverted and stratified boundary layer simulations. However, vertically resolved chemical observations are required to apply the Geyer and Stutz (2004) method.

As MISTRA is a 1-D model, horizontal mixing is not included. This lack of horizontal mixing ensures that column-integrated abundances conserve mass, allowing the analysis shown here, while still explicitly allowing vertical mixing that is necessary to consider the competition between surface and aloft chemical processes. Horizontal mixing over the duration of the model runs will depend strongly on the prevailing synoptic situation so that a quantification of the effect of horizontal mixing is not possible. Horizontal mixing with background ozone would lead to less limitation of Reactions (R1) and (R2) and more efficient removal of NO<sub>x</sub>.

Aerosol particles in the simulations were represented as purely aqueous constituents. With respect to frozen water, observations by LIDAR in Fairbanks indicate presence of super-cooled droplets in high-latitude environments at temperatures as low as 240 K, suggesting aqueous-phase aerosols are present in temperatures well below the freezing temperature of water (Fochesatto et al., 2005). The freezing of particles would have complex and currently poorly understood effects on reactivity. However, freezing could potentially occur on the 2-day timescale, implying that more study of the structure and reactivity of ice particles is needed.

Field observations have shown that the reactive uptake coefficient parameterization of (Bertram and Thornton, 2009) often results in  $\gamma$  values larger than observed in the field, which has been associated with organic aerosol content (Bertram et al., 2009; Riedel et al., 2012; Ryder et al., 2014). We had no observational constraints on the properties of the organic matter in the aerosol particles (internal/external mixing state, O:C ratio, etc.), so we could not enhance the  $\gamma$  calculation model. However,  $\gamma$  observed under wintertime conditions in the study of Wagner et al. (2013) was comparable to and sometimes exceeded the calculation method used here, possibly indicating that the Bertram and Thorn-

ton (2009) model is reasonably accurate under the conditions simulated here. The significant uncertainties that exist in the proper calculation of  $\gamma$  need further study, and the study we report here indicates that airborne observations of N<sub>2</sub>O<sub>5</sub> should be particularly sensitive to  $\gamma$  and aerosol particle properties.

## 6 Conclusions

Simulations have shown that approximately two-thirds of NO<sub>x</sub> is lost in the 2 days after emission in high-latitude winter conditions mostly through the dark oxidation pathway. Observed pollution fluxes commonly produce a reduced environment with excess NO and near-zero ozone, slowing secondary oxidation chemistry that removes NO<sub>x</sub>. The fraction of emitted NO<sub>x</sub> that remains in the atmosphere was found to be most sensitive to the NO emission flux and temperature. Winter months with relatively warm temperatures and high mixing heights are likely to have the greatest nitrate aerosol particulate loading. Alternatively, cold days with low mixed layers are likely to have the greatest dry deposition rates and greatest local nitrogen deposition impact. Dry deposition rates of N<sub>2</sub>O<sub>5</sub> were found to be most sensitive to aerosol surface area and dry deposition velocity, illustrating the competition between dry deposition and aerosol reactivity for the removal of N<sub>2</sub>O<sub>5</sub>. Due to ground contact only occurring in the bottom model layer, greater amounts of total emitted NO<sub>x</sub> were removed from the column via aerosol particle reactions (38 %) than through dry deposition (17 %) two days after emission in the base case scenario. Modeled abundances of N<sub>2</sub>O<sub>5</sub> showed diurnal variations of over 1000 % and positive vertical gradients from the snowpack, showing the need for further study to understand vertical distribution of the emission plume and estimate potential impacts.

*Acknowledgements.* The authors would like to thank NOAA for use of the Ferret program for analysis of model output and UCAR for the use of NCL plotting software, which was used to generate the figures in this manuscript. The authors would like to thank Deanna Huff and Barbara Trost with the Alaska Department of Environmental Conservation and Jim Connor with the Fairbanks North Star Borough Air Quality Division for collaboration and providing observational data. Thanks to Catherine Cahill, Tom Trainor, and the two reviewers for helpful comments. This project was funded by the NSF under grant ATM-0926220. We also thank Flora Grabowski at the Keith Mather Library in the Geophysical Institute for supporting open access publication of this article.

Edited by: R. Sander

## References

- ACRC: Alaska Climate Research Center Climate data for Fairbanks, AK, <http://climate.gi.alaska.edu/Climate/Location/TimeSeries/Fairbanks.html>, 2011.
- ADEC: Alaska Department of Environmental Conservation Supplemental information: PM<sub>2.5</sub> Designation and Boundary Recommendations, [http://dec.alaska.gov/air/doc/PM25\\_info.pdf](http://dec.alaska.gov/air/doc/PM25_info.pdf), 2007.
- ADEC: Alaska Department of Environmental Conservation Fairbanks non-attainment area boundary comments. Emissions Inventory 2005, [http://www.dec.state.ak.us/air/doc/DEC\\_EPA\\_Fbks\\_NA\\_20oct08.pdf](http://www.dec.state.ak.us/air/doc/DEC_EPA_Fbks_NA_20oct08.pdf), 2008.
- Akagi, S. K., Yokelson, R. J., Wiedinmyer, C., Alvarado, M. J., Reid, J. S., Karl, T., Crouse, J. D., and Wennberg, P. O.: Emission factors for open and domestic biomass burning for use in atmospheric models, *Atmos. Chem. Phys.*, 11, 4039–4072, doi:10.5194/acp-11-4039-2011, 2011.
- Anderson, P. S. and Neff, W. D.: Boundary layer physics over snow and ice, *Atmos. Chem. Phys.*, 8, 3563–3582, doi:10.5194/acp-8-3563-2008, 2008.
- Anttila, T., Kiendler-Scharr, A., Tillmann, R., and Mentel, T. F.: On the Reactive Uptake of Gaseous Compounds by Organic-Coated Aqueous Aerosols: Theoretical Analysis and Application to the Heterogeneous Hydrolysis of N<sub>2</sub>O<sub>5</sub>, *The Journal of Physical Chemistry A*, 110, 10435–10443, doi:10.1021/jp062403c, <http://pubs.acs.org/doi/abs/10.1021/jp062403c>, PMID: 16942049, 2006.
- Apodaca, R., Huff, D., and Simpson, W.: The role of ice in N<sub>2</sub>O<sub>5</sub> heterogeneous hydrolysis at high latitudes, *Atmos. Chem. Phys.*, 8, 7451–7463, doi:10.5194/acp-8-7451-2008, 2008.
- ARCTAS: Arctic Research of the Composition of the Troposphere by Aircraft and Satellites NASA DC-8 aircraft data, <http://www-air.larc.nasa.gov/cgi-bin/arctas-c>, 2008.
- Ayers, J. D. and Simpson, W. R.: Measurements of N<sub>2</sub>O<sub>5</sub> near Fairbanks, Alaska, *J. Geophys. Res.*, 111, D14309, doi:10.1029/2006JD007070, 2006.
- Bertram, T. and Thornton, J.: Toward a general parameterization of N<sub>2</sub>O<sub>5</sub> reactivity on aqueous particles: The competing effects of particle liquid water, nitrate and chloride, *Atmos. Chem. Phys.*, 9, 8351–8363, doi:10.5194/acp-9-8351-2009, 2009.
- Bertram, T. H., Thornton, J. A., Riedel, T. P., Middlebrook, A. M., Bahreini, R., Bates, T. S., Quinn, P. K., and Coffman, D. J.: Direct observations of N<sub>2</sub>O<sub>5</sub> reactivity on ambient aerosol particles, *Geophys. Res. Lett.*, 36, n/a–n/a, doi:10.1029/2009GL040248, <http://dx.doi.org/10.1029/2009GL040248>, 2009.
- Bott, A., Trautmann, T., and Zdunkowski, W.: A numerical model of the cloud topped planetary boundary layer: Radiation, turbulence and spectral microphysics in marine stratus, *Q. J. R. Meteorol. Soc.*, 122, 635–667, 1996.
- Brandt, C. and van Eldik, R.: Transition metal-catalyzed oxidation of sulfur (IV) oxides Atmospheric-relevant processes and mechanisms, *Chem. Rev.*, 95, 119–190, 1995.
- Brown, S., Stark, H., Ryerson, T., Williams, E., Nicks, D., Trainer, M., Fehsenfeld, F., and Ravishankara, A.: Nitrogen oxides in the nocturnal boundary layer: Simultaneous in situ measurements of NO<sub>3</sub>, N<sub>2</sub>O<sub>5</sub>, NO<sub>2</sub>, NO, and O<sub>3</sub>, *J. Geophys. Res.*, 108, 2917, doi:10.1029/2002JD002917, 2003.
- Brown, S., Dubé, W., Osthoff, H., Stutz, J., B., R. T., Wollny, A. G., Brock, C. A., Warneke, C., de Gouw, J. A., Atlas, E., Neuman, J. A., Holloway, J. S., Lerner, B. M., Williams, E. J., Kuster, W. C., Goldan, P. D., Angevine, W. M., Trainer, M., Fehsenfeld, F. C., and Ravishankara, A. R.: Vertical profiles in NO<sub>3</sub> and N<sub>2</sub>O<sub>5</sub> measured from an aircraft: Results from the NOAA P-3 and surface platforms during the New England Air Quality Study 2004, *J. Geophys. Res.*, 112, doi:10.1029/2007JD008883, 2007a.
- Brown, S. S., Dubé, W. P., Osthoff, H. D., Wolfe, D. E., Angevine, W. M., and Ravishankara, A. R.: High resolution vertical distributions of NO<sub>3</sub> and N<sub>2</sub>O<sub>5</sub> through the nocturnal boundary layer, *Atmos. Chem. Phys.*, 7, 139–149, doi:10.5194/acp-7-139-2007, 2007b.
- Brown, S. S., Dubé, W. P., Fuchs, H., Ryerson, T. B., Wollny, A. G., Brock, C. A., Bahreini, R., Middlebrook, A. M., Neuman, J. A., Atlas, E., Roberts, J. M., Osthoff, H. D., Trainer, M., Fehsenfeld, F. C., and Ravishankara, A. R.: Reactive uptake coefficients for N<sub>2</sub>O<sub>5</sub> determined from aircraft measurements during the Second Texas Air Quality Study: Comparison to current model parameterizations, *J. Geophys. Res.-Atmos.*, 114, n/a–n/a, doi:10.1029/2008JD011679, <http://dx.doi.org/10.1029/2008JD011679>, 2009.
- Chang, W. L., Bhavsar, P. V., Brown, S. S., Riemer, N., Stutz, J., and Dabdub, D.: Heterogeneous Atmospheric Chemistry, Ambient Measurements, and Model Calculations of N<sub>2</sub>O<sub>5</sub>: A Review, *Aerosol Sci. Technol.*, 45, 665–695, doi:10.1080/02786826.2010.551672, <http://dx.doi.org/10.1080/02786826.2010.551672>, 2011.
- Dentener, F. J. and Crutzen, P. J.: Reaction of N<sub>2</sub>O<sub>5</sub> on Tropospheric Aerosols: Impact on the Global Distributions of NO<sub>x</sub>, O<sub>3</sub>, and OH, *J. Geophys. Res.*, 98, 7149–7163, 1993.
- ESRL: Earth System Research Laboratory, Global Monitoring Division, Surface ozone, in-situ hourly averages, Barrow, AK, [http://www.esrl.noaa.gov/gmd/dv/data/index.php?site=brw&category=Ozone&parameter\\_name=SurfBOzone](http://www.esrl.noaa.gov/gmd/dv/data/index.php?site=brw&category=Ozone&parameter_name=SurfBOzone), 2011.
- Evans, M. J. and Jacob, D. J.: Impact of new laboratory studies of N<sub>2</sub>O<sub>5</sub> hydrolysis on global model budgets of tropospheric nitrogen oxides, ozone, and OH, *Geophys. Res. Lett.*, 32, n/a–n/a, doi:10.1029/2005GL022469, <http://dx.doi.org/10.1029/2005GL022469>, 2005.
- Fenn, M., Baron, J., Allen, E., Rueth, H., Nydick, K., Geiser, L., Bowman, W., Sickman, J., Meixner, T., and Johnson, D.: Ecological effects of nitrogen deposition in the western United States, *BioScience*, 53, 404–420, 2003.
- Finlayson-Pitts, B. and Pitts, J.: *Chemistry of the Upper and Lower Atmosphere*, Academic Press, 2000.
- Fochesatto, J., Collins, R., Yue, J., Cahill, C., and Sassen, K.: Compact eye-safe backscatter lidar for aerosol studies in urban polar environment, Vol. 5887, 58870U–58870U–9, SPIE, 2005.
- Gaston, C. J., Thornton, J. A., and Ng, N. L.: Reactive uptake of N<sub>2</sub>O<sub>5</sub> to internally mixed inorganic and organic particles: the role of organic carbon oxidation state and inferred organic phase separations, *Atmos. Chem. Phys.*, 14, 5693–5707, doi:10.5194/acp-14-5693-2014, 2014.
- Geyer, A. and Stutz, J.: Vertical profiles of NO<sub>3</sub>, N<sub>2</sub>O<sub>5</sub>, O<sub>3</sub>, and NO<sub>x</sub> in the nocturnal boundary layer: 2 Model studies on the altitude dependence of composition and chemistry, *J. Geophys. Res.*, 109, D12307, doi:10.1029/2003JD004211, 2004.
- Graedel, T. E. and Keene, W. C.: Tropospheric budget of reactive chlorine, *Global Biogeochem. Cycles*, 9, 47, doi:10.1029/94GB03103, 1995.

- Hanson, D. R. and Ravishankara, A. R.: The Reaction Probabilities of ClONO<sub>2</sub> and N<sub>2</sub>O<sub>5</sub> on 40 to 75% Sulfuric Acid Solutions, *J. Geophys. Res.*, 96, 17307–17314, doi:10.1029/91JD01750, 1991.
- Hoffman, M. R. and Boyce, S. D.: Catalytic autooxidation of aqueous sulfur dioxide in relationship to atmospheric systems, *Adv. Environ. Sci. Technol.*, 12, 148–189, 1983.
- Huff, D. M., Joyce, P. L., Fochesatto, G. J., and Simpson, W. R.: Deposition of dinitrogen pentoxide, N<sub>2</sub>O<sub>5</sub>, to the snowpack at high latitudes, *Atmos. Chem. and Phys.*, 11, 4929–4938, doi:10.5194/acp-11-4929-2011, 2011.
- Jaenicke, R.: Tropospheric aerosols, chap. Chapter 1: Aerosol-Cloud-Climate Interactions, 1993.
- Kramm, G., Dlugi, R., Dollard, G., Foken, T., Mölders, N., Müller, H., Seiler, W., and Sievering, H.: On the dry deposition of ozone and reactive nitrogen species, *Atmos. Environ.*, 29, 3209–3231, doi:10.1016/1352-2310(95)00218-N, 1995.
- Landgraf, J. and Crutzen, P.: An Efficient Method for “On-Line” Calculations of Photolysis and Heating Rates, *J. Atmos. Sci.*, 55, 863–878, 1998.
- Mentel, T. F., Sohn, M., and Wahner, A.: Nitrate effect in the heterogeneous hydrolysis of dinitrogen pentoxide on aqueous aerosols, *Phys. Chem. Chem. Phys.*, 2, 5451–5457, doi:10.1039/A905338G, 1999.
- NCDC: National Climate Data Center, Relative humidity from Fairbanks, AK station (PAFA), <ftp://ftp.ncdc.noaa.gov/pub/data/asos-fivemin/6401-2009/>, 2011.
- Nowak, J. B., Neuman, J. A., Bahreini, R., Middlebrook, A. M., Holloway, J. S., McKeen, S. A., Parrish, D. D., Ryerson, T. B., and Trainer, M.: Ammonia sources in the California South Coast Air Basin and their impact on ammonium nitrate formation, *Geophys. Res. Lett.*, 39, n/a–n/a, doi:10.1029/2012GL051197, <http://dx.doi.org/10.1029/2012GL051197>, 2012.
- Osthoff, H., Roberts, J., Ravishankara, A., Williams, E., Lerner, B., Sommariva, R., Bates, T., Coffman, D., Quinn, P., Dibb, J., Stark, H., Burkholder, J. B., Talukdar, R. K., Meagher, J., Fehsenfeld, F. C., and Brown, S. S.: High levels of nitryl chloride in the polluted subtropical marine boundary layer, *Nat. Geosci.*, 1, doi:10.1038/ngeo177, 2008.
- Pechtl, S., Lovejoy, E. R., Burkholder, J. B., and von Glasow, R.: Modeling the possible role of iodine oxides in atmospheric new particle formation, 6, 503–523, 2006.
- Piot, M. and von Glasow, R.: The potential importance of frost flowers, recycling on snow, and open leads for ozone depletion events, *Atmos. Chem. Phys.*, 8, 2437–2467, doi:10.5194/acp-8-2437-2008, 2008.
- Riedel, T. P., Bertram, T. H., Ryder, O. S., Liu, S., Day, D. A., Russell, L. M., Gaston, C. J., Prather, K. A., and Thornton, J. A.: Direct N<sub>2</sub>O<sub>5</sub> reactivity measurements at a polluted coastal site, *Atmospheric Chemistry and Physics*, 12, 2959–2968, doi:10.5194/acp-12-2959-2012, <http://www.atmos-chem-phys.net/12/2959/2012/>, 2012.
- Riemer, N., Vogel, H., Vogel, B., Anttila, T., Kiendler-Scharr, A., and Mentel, T. F.: Relative importance of organic coatings for the heterogeneous hydrolysis of N<sub>2</sub>O<sub>5</sub> during summer in Europe, *J. Geophys. Res.-Atmos.*, 114, n/a–n/a, doi:10.1029/2008JD011369, <http://dx.doi.org/10.1029/2008JD011369>, 2009.
- Ryder, O. S., Ault, A. P., Cahill, J. F., Guasco, T. L., Riedel, T. P., Cuadra-Rodriguez, L. A., Gaston, C. J., Fitzgerald, E., Lee, C., Prather, K. A., and Bertram, T. H.: On the Role of Particle Inorganic Mixing State in the Reactive Uptake of N<sub>2</sub>O<sub>5</sub> to Ambient Aerosol Particles, *Environ. Sci. Technol.*, 48, 1618–1627, doi:10.1021/es4042622, <http://pubs.acs.org/doi/abs/10.1021/es4042622>, 2014.
- Seinfeld, J. H. and Pandis, S. N.: *Atmospheric Chemistry and Physics*, 2nd ed., 2006.
- Sommariva, R. and von Glasow, R.: Multi-phase halogen chemistry in the tropical Atlantic Ocean, *Environ. Sci. Technol.*, 46, 10429–10437, 2012.
- State of Alaska: Measurements of NO<sub>x</sub> and SO<sub>2</sub> from downtown Fairbanks, 2008–2009, personal communication with Alaska Department of Environmental Conservation, 2011, 2008.
- State of Alaska: Aerosol particle composition from downtown Fairbanks, 2006–2010, personal communication with Alaska Department of Environmental Conservation, 2011.
- Thornton, J. A., Kercher, J. P., Riedel, T. P., Wagner, N. L., Cozic, J., Holloway, J. S., Dubé, W. P., Wolfe, G. M., Quinn, P. K., Middlebrook, A. M., Alexander, B., and Brown, S. S.: A large atomic chlorine source inferred from mid-continental reactive nitrogen chemistry, *Nature*, 464, 271–274, doi:10.1038/nature08905, 2010.
- TOMS: Total Ozone Mapping Spectrometer (TOMS). What is the total column ozone over your house?, [http://toms.gsfc.nasa.gov/teacher/ozone\\_overhead\\_v8.html](http://toms.gsfc.nasa.gov/teacher/ozone_overhead_v8.html), 2011.
- Van Doren, J., Watson, L., Davidovits, P., Worsnop, D., Zahniser, M., and Kolb, C.: Uptake of N<sub>2</sub>O<sub>5</sub> and HNO<sub>3</sub> by aqueous sulfuric acid droplets, *J. Phys. Chem.*, 95, 1684–1689, 1991.
- von Glasow, R., Sander, R., Bott, A., and Crutzen, P.: Modeling halogen chemistry in the marine boundary layer 1. Cloud-free MBL, *J. Geophys. Res.*, 107, 4352, doi:10.1029/2001JD000942, 2002.
- Wagner, N. L., Riedel, T. P., Young, C. J., Bahreini, R., Brock, C. A., Dubé, W. P., Kim, S., Middlebrook, A. M., Öztürk, F., Roberts, J. M., Russo, R., Sive, B., Swarthout, R., Thornton, J. A., VandenBoer, T. C., Zhou, Y., and Brown, S. S.: N<sub>2</sub>O<sub>5</sub> uptake coefficients and nocturnal NO<sub>2</sub> removal rates determined from ambient wintertime measurements, *J. Geophys. Res.-Atmos.*, 118, 9331–9350, doi:10.1002/jgrd.50653, 2013.
- Wesely, M.: Parameterization of surface resistances to gaseous dry deposition in regional-scale numerical models, *Atmos. Environ.*, 23, 1293–1304, 1989.
- Wesely, M. and Hicks, B.: A review of the current status of knowledge on dry deposition, *Atmos. Environ.*, 34, 2261–2282, 2000.
- Wood, E., Bertram, T., and Wooldridge, P.: Measurements of N<sub>2</sub>O<sub>5</sub>, NO<sub>2</sub>, and O<sub>3</sub> east of the San Francisco Bay, *Atmos. Chem. Phys.*, 5, 483–491, doi:10.5194/acp-5-483-2005, 2005.
- Yokelson, R. J., Griffith, D. W. T., and Ward, D. E.: Open-path Fourier transform infrared studies of large-scale laboratory biomass fires, *J. Geophys. Res.*, 101, 21067–21080, doi:10.1029/96JD01800, 1996.
- Yokelson, R. J., Susott, R., Ward, D. E., Reardon, J., and Griffith, D. W. T.: Emissions from smoldering combustion of biomass measured by open-path Fourier transform infrared spectroscopy, *J. Geophys. Res.*, 102, 18865–18877, doi:10.1029/97JD00852, 1997.